The all-seeing eye of resonant Auger electron spectroscopy: a study on aqueous solution using tender x-rays

Tsveta Miteva,[*,†] Nikolai V. Kryzhevoi,[‡] Nicolas Sisourat,[†] Christophe Nicolas,[¶] Wandared Pokapanich,[§] Thanit Saisopa,[‖] Prayoon Songsiriritthigul,[‖] Yuttakarn Rattanachai,[⊥] Andreas Dreuw,[#] Jan Wenzel,[#] Jérôme Palaudoux,[†] Gunnar Öhrwall,[@] Ralph Püttner,[△] Lorenz S. Cederbaum,[‡] Jean-Pascal Rueff,[†,¶] and Denis Céolin[*,¶]

†*Sorbonne Université, CNRS, Laboratoire de Chimie Physique Matière et Rayonnement, UMR 7614, F-75005 Paris, France*

‡*Theoretische Chemie, Physikalisch-Chemisches Institut, Universität Heidelberg, Im Neuenheimer Feld 229, D-69120 Heidelberg, Germany*

¶*Synchrotron SOLEIL, l'Orme des Merisiers, Saint-Aubin, F-91192 Gif-sur-Yvette Cedex, France*

§*Faculty of Science, Nakhon Phanom University, Nakhon Phanom 48000, Thailand*

‖*School of Physics, Suranaree University of Technology, Nakhon Ratchasima 30000, Thailand*

⊥*Department of Applied Physics, Faculty of Sciences and Liberal Arts, Rajamangala University of Technology Isan, Nakhon Ratchasima 30000, Thailand*

#*Interdisciplinary Center for Scientific Computing, Ruprecht-Karls University, Im Neuenheimer Feld 205A, D-69120 Heidelberg, Germany*

@*MAX IV Laboratory, Lund University, P.O. Box 118, SE-22100 Lund, Sweden*

△*Fachbereich Physik, Freie Universität Berlin, Arnimallee 14, D-14195, Berlin, Germany*

E-mail: tsveta.miteva@upmc.fr; denis.ceolin@synchrotron-soleil.fr

Abstract

X-ray absorption and Auger electron spectroscopies are demonstrated to be powerful tools to unravel the electronic structure of solvated ions. In this work for the first time we use a combination of these methods in the tender x-ray regime. This allowed us to address electronic transitions including deep core levels and to probe environmental effects, specifically in the bulk of solutions since the Auger electrons created by deep core levels possess large mean free paths. In the considered exemplary aqueous KCl solution the solvated isoelectronic K^+ and Cl^- ions exhibit notably different Auger electron spectra as a function of the photon energy. The differences appear due to dipole forbidden transitions in aqueous K^+ whose occurrence, according to the performed *ab initio* calculations, becomes possible only in the presence of solvent water molecules.

Graphical TOC Entry

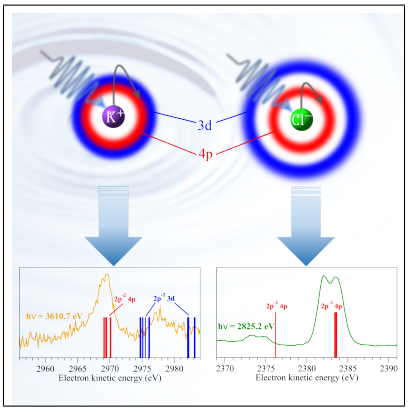

Keywords

Solvated ions, Auger electron spectroscopy, x-ray absorption spectroscopy

Understanding how atoms or molecules respond to irradiation with x-rays gives insight into the structure of solutions (Ref.[1] and references therein), and the mechanisms of radiation damage[2–4]. Depending on the photon energy, the absorption of an x-ray photon results in the population of core excited or core ionized states. The relaxation of these highly energetic states involves an ultrafast cascade of intraatomic processes, such as radiative and Auger decays, and it depends on the character of the initially populated states[5–12]. Furthermore, if the initially excited or ionized species is embedded in an environment, interatomic processes are possible[4,13–16].

X-ray absorption spectroscopy (XAS) is a powerful tool to study the nearest environment of atoms in gas phase as it probes core excited states below threshold which are highly sensitive to the surrounding. However, for atoms and molecules in liquid or solid phase, these core excited states overlap significantly in the XAS spectra inhibiting access to the available information (REF). This drawback can be overcome by detecting the electrons resulting from the subsequent resonant Auger decay and thus using this complementary information to separate the overlapping states[17]. In a liquid jet, this method applied to shallow core holes (like O 1s of the water molecule) mainly provides information from sites close to the liquid-solid interface, due to the short mean free path of the low-kinetic-energy Auger electrons. With a recently commissioned setup using tender X-rays [18,19] we are now able to reach deeper core levels resulting in much faster Auger electrons, and as a consequence, one can have a significantly deeper look into the liquid.

In this work we used Auger electron spectroscopy (AES) together with XAS in the tender x-ray regime to study the electronic decay processes following x-ray absorption of aqueous potassium chloride at the K-edges of both K^+ and Cl^-. In particular, we demonstrate experimentally that at photon energies below the K-edges of the two ions, core excited states are populated. These states undergo resonant Auger decay within less than 1 fs[16]. Although the K^+ and Cl^- ions are isoelectronic, they have different fingerprints in the resonant Auger spectra. We demonstrate that these differences result from different electronic structures of

the two ions, thus confirming that the combination of XAS and AES techniques is a sensitive probe of the electronic structure of solutions.

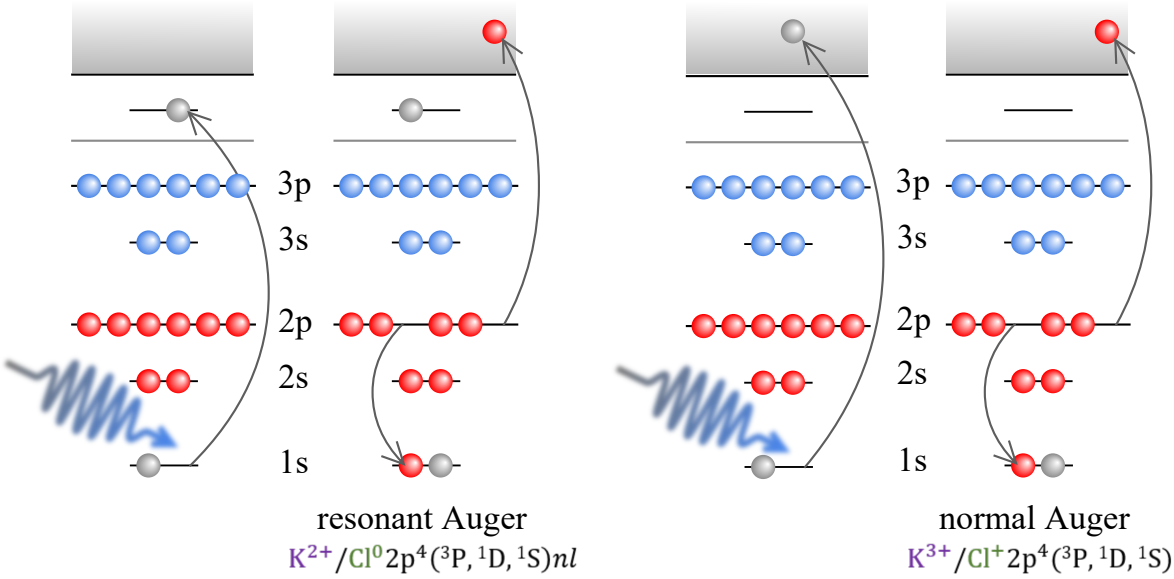

Figure 1: Schematic representation of the resonant (left) and normal (right) Auger processes of the isoelectronic K^+ and Cl^- ions.

The resonant and normal Auger processes which we investigated in this work are schematically shown on Fig. 1. The $KL_{2,3}L_{2,3}$ normal Auger decay following K-shell ionization of aqueous K^+ and Cl^- populates the $2p^{-2}(^3P, ^1D, ^1S)$ final states. The transitions to ^3P final states have a very low intensity since they are forbidden from parity conservation rules. In the case of K^+_{aq} the maxima of the ^1S and ^1D $KL_{2,3}L_{2,3}$ Auger lines at photon energy $h\nu = 3616.0\,eV$ are located at kinetic energy $E_{kin} = 2958.0\,eV$ and $2968.5\,eV$, respectively (Fig. 2 (c)). For Cl^-_{aq}, the lines corresponding to the Cl^+ $2p^{-2}(^1S)$ and (^1D) states are located at $E_{kin} = 2373.1\,eV$ and $2382.0\,eV$ for a photon energy of $2830.0\,eV$ (Fig. 3 (c)).

The $KL_{2,3}L_{2,3}$ normal Auger lines may be shifted to higher kinetic energies and also disperse with photon energy close to threshold due to energy exchange between the photoelectron and Auger electron called post-collision interaction (PCI)[20,21]. In our spectra, the PCI effect is manifested as an asymmetric tail of the main peaks at photon energies $3616\,eV$ in the case of K^+, and $2830\,eV$ in the case of Cl^-, and as a shift of $\sim 1\,eV$ of the maxima

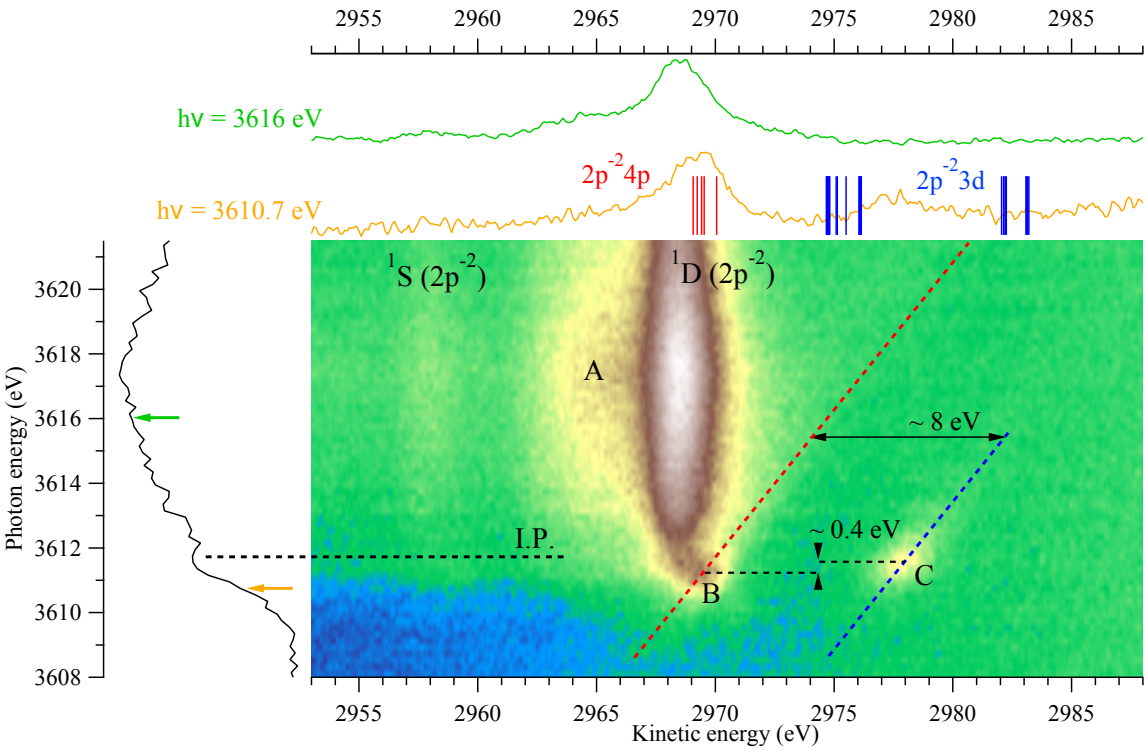

Figure 2: (a) 2D map showing the kinetic energy of the electrons emitted in $KL_{2,3}L_{2,3}$ Auger decay vs the photon energy in the vicinity of the K-edge of aqueous K^+. The features A, B and C are discussed in the text. (b) Experimental partial electron yield spectrum of K^+ obtained after integrating over the kinetic energies of the Auger electrons. (c) Auger spectra at photon energies 3610.7 eV and 3616 eV. The vertical bars in the resonant Auger spectrum measured at 3610.7 eV indicate the spectator Auger energies of the calculated doublet $2p^{-2}$ 3d (blue) and $2p^{-2}4p$ (red) states of $K^+(H_2O)_6$.

towards lower kinetic energies as compared to the spectra reported in[16]. More details are given in the SI.

Finally, the normal Auger ^{1}D main line of K^+ differs from that of Cl^- by the presence of a large shoulder on the low kinetic energy side at $E_{kin} \cong 2965$ eV, feature A (Fig. 2(a)). This shoulder is attributed to electron transfer from the solvent water molecules to the unoccupied 3d orbitals of $K^{3+}(2p^{-2})$ resulting in $K^{2+}(2p^{-2}3d)W^{-1}$[16]. In the case of Cl^-, there is no experimental evidence of such intense electron transfer processes.

The pre-edge regions of the XAS spectra of K^+ and Cl^- shown in Figs. 2(b) and 3(b)

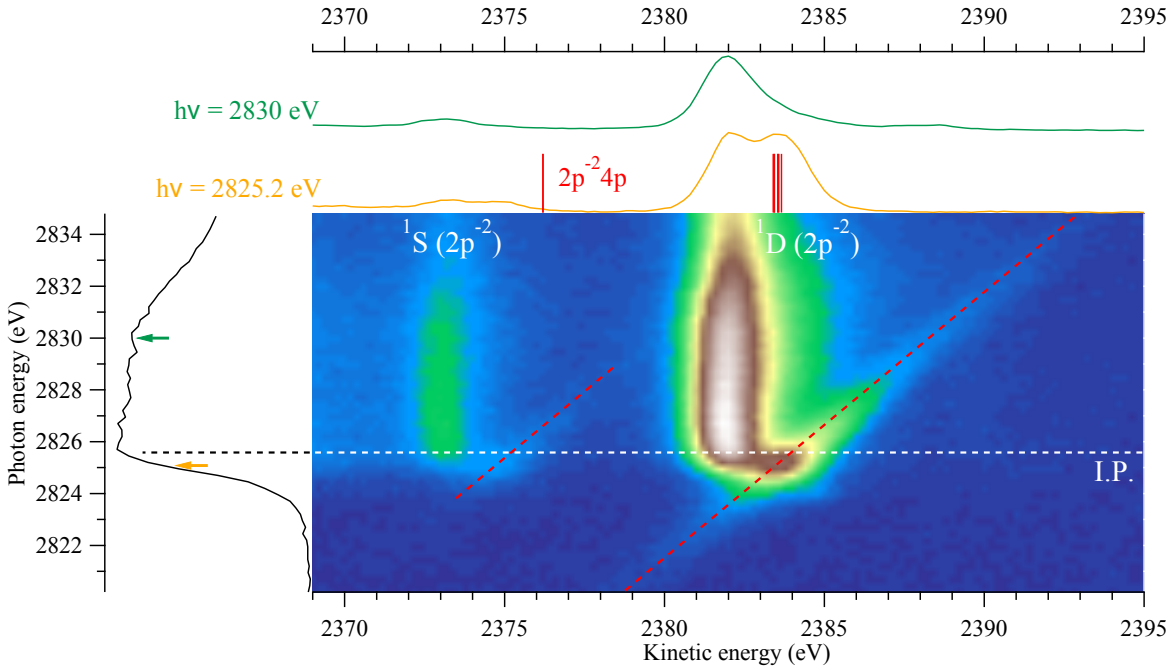

Figure 3: (a) 2D map showing the kinetic energy of the electrons emitted in $KL_{2,3}L_{2,3}$ Auger decay vs the photon energy in the vicinity of the K-edge of aqueous Cl^-. (b) Experimental partial electron yield spectrum of Cl^- obtained after integrating over the kinetic energies of the Auger electrons. (c) Auger spectra at photon energies 2825.2 eV and 2830.0 eV. The vertical bars in the resonant Auger spectrum at 2825.2 eV indicate the the spectator Auger energies of the calculated doublet $2p^{-2}4p$ states of $Cl^-(H_2O)_6$.

do not show any clear indication of core excited states due to their lifetime broadening and energetic proximity to the ionization threshold. Instead these states can be identified by their resonant Auger features, which disperse with photon energy and thus significantly differ from the normal Auger ones. In the 2D map of Cl^- (Fig. 3) there are two dispersive resonant Auger features indicated with diagonal dashed lines. Both of them have a maximum at photon energy $h\nu = 2825.2$ eV, which is in good agreement with the position of the Cl^- $1s^{-1}4p$ excitation determined from Cl K-edge XAS experiments on hydrated Mg and Sr chlorides[22] and metal-chloride complexes[23]. These features have $E_{\mathrm{kin}} = 2374.6$ and 2383.4 eV, respectively, which demonstrates that they are related to the ^{1}S and ^{1}D main lines. In the case of K^+, the dispersive line related to the ^{1}S main line cannot be clearly

identified due to the presence of strong background. Instead two dispersive features related to the ^{1}D main line are observed denoted as B and C on Fig. 2(a). Feature B exhibits a maximum at hν = 3611.2 eV and E_{kin} = 2969.2 eV. The additional feature C appears at hν = 3611.6 eV and E_{kin} = 2978.1 eV, thus it is separated by approximately 400 meV in photon energy and 8.3 eV in kinetic energy from the maximum of feature B. The positions of these two core excited states are close to the energy of the $1s^{-1}4p$ excitation of gas-phase K^+ at 3610.7 eV[24].

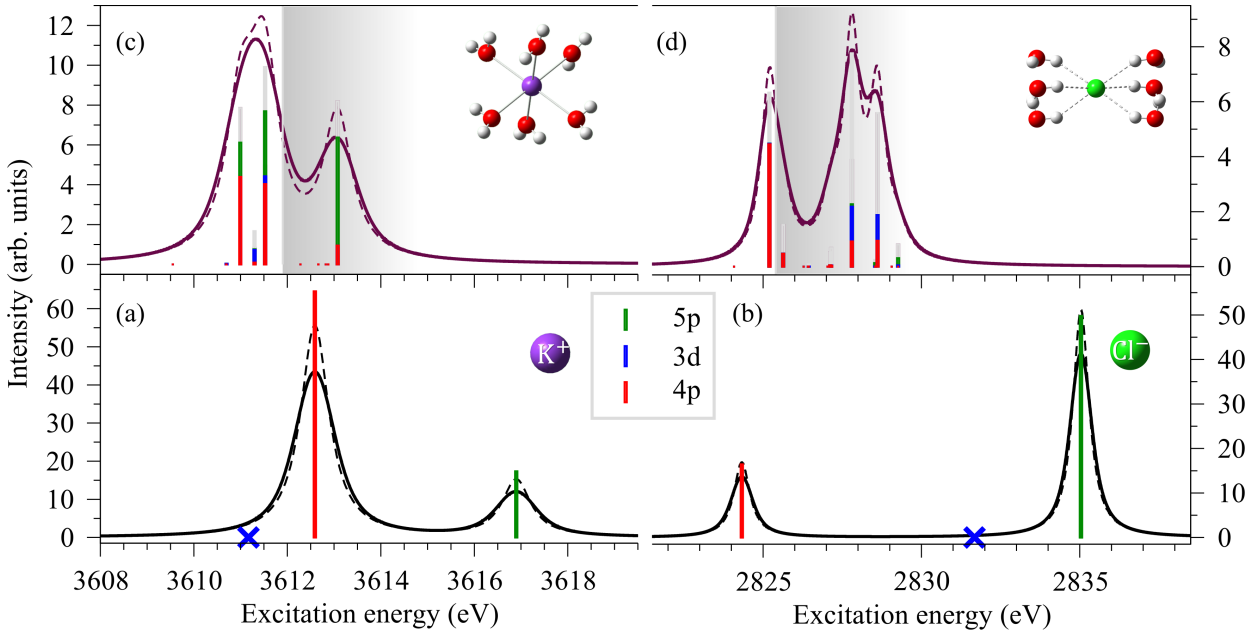

Figure 4: XAS spectra of the lowest K-shell resonant transitions in the isolated K^+ (a) and Cl^- (b) ions and their 6-coordinated clusters ((c) and (d)). For comparison with the experiment, the theoretical stick spectra are convolved with a Lorentzian of FWHM 0.74 eV and 0.62 eV representing the lifetime broadening of K^+ and Cl^-[25] (dashed lines) and a Voigt profile (solid line) to account for both the lifetime and the experimental broadening (see text). The colors in the stick spectrum represent the projections of the singly-occupied natural orbitals (SONOs) of the core excited 6-coordinated clusters on the basis of SONOs belonging to the $1s^{-1}3d$, $1s^{-1}4p$, and $1s^{-1}5p$ states of the isolated ions. The remaining contributions from higher-lying atomic core excitations or from excitations to the solvent molecules are depicted as grey sticks. The theoretical XAS spectra of both K^+ and Cl^- were shifted to higher photon energies such that the energies of the lowest core excited states correspond to the experimentally determined ones. The experimental ionization thresholds are depicted as grey boxes.

In order to rationalize the pre-edge region of the experimental XAS spectra and the

differences in the AES spectra of K^+_{aq} and Cl^-_{aq}, we computed the lowest core excited states of the isolated K^+ and Cl^- ions and their hexa-coordinated clusters (Fig. 4). The lowest peak in the XAS spectra of the isolated ions corresponds to the dipole allowed $1s^{-1}4p$ state followed by the second bright state, $1s^{-1}5p$, which is higher in energy by 4.3 eV and 10.8 eV in K^+ and Cl^-, respectively. For both ions, the energy positions of the dipole forbidden $1s^{-1}3d$ states are indicated as blue crosses. It is noteworthy that the positions of the $1s^{-1}4p$ and $1s^{-1}3d$ states are inverted in K^+ and Cl^-, and moreover, the splitting between these states is about two times smaller in K^+. These findings are crucial for understanding the Auger spectra of the two ions as shown below. Upon addition of water molecules, the degeneracy of the states is lifted and they interact with other states of the ion or the neighboring water molecules (Fig. 4(c),(d)). Thus, dipole forbidden states acquire intensity in the cluster. A similar effect was observed in the XAS spectra of microsolvated clusters of Na^+ and Mg^{2+} [26]. Details on the calculations of the XAS spectra are given in the SI.

Further by comparing the experimental and theoretical XAS spectra, we assume that only the states of the lowest peak in the theoretical XAS spectra are populated in the experiment. In the 6-coordinated K^+ cluster the lowest peak in the spectrum contains three states. The lowest and highest lying states are split by approximately 0.5 eV and they have mixed 4p and 5p character while the low intensity state in between has a predominantly $1s^{-1}3d$ character. Since the dispersive feature B appears at low excitation energies, we assume that it is produced in the resonant Auger decay of the lowest core excited states of K^+ of predominantly $1s^{-1}4p$ character. Moreover, we can attribute the feature C to the resonant Auger decay of the low intensity dipole forbidden $1s^{-1}3d$ state. Thus, we explain both the energy splitting of $\sim$400 meV photon energy of B and C, and the fact that island C has lower intensity than B (Fig. 2). In the hexa-coordinated cluster of Cl^-, the solvent molecules have little influence on the position and character of the first state – it has mainly Cl^- $1s^{-1}4p$ character with some admixture of states of the nearest water molecules. Consequently, we attribute the two dispersive features associated with the ^1S and ^1D main

lines on the 2D map of Cl^- to the resonant Auger decay of this core excited state.

To fully characterize the dispersive features on the experimental 2D maps, we also computed the lowest doublet states of the type $K^{2+}[2p^{-2}nl](H_2O)_6$ and $Cl^0[2p^{-2}nl](H_2O)_6$. These states are the final states of the spectator Auger decay. The latter is the predominant decay process for the low-lying core excited states in argon[27], which is isoelectronic to K^+ and Cl^-. The energy positions of the states are adjusted to the kinetic-energy scale of the Auger spectra of both ions such that the lowest $2p^{-2}(^1D)4p$ states coincide with the maxima of the dipsersive features related to the ^1D main line. The results are shown as bars in Figs. 2(c) and 3(c). As can be seen from the bars overlapping the Auger spectrum recorded at $h\nu = 3610.7\,eV$ (Fig. 2(c)), the lowest $2p^{-2}4p$ states of $K^+(H_2O)_6$ are lower in energy by $\sim$5 and 12-13 eV than two groups of $2p^{-2}3d$ states. Thus, the transitions to the group of $2p^{-2}3d$ final states at $E_{kin} \cong 2975\,eV$ are closer to the kinetic energy of island C. Consequently, we attribute this dispersive feature as originating from the resonant Auger decay of the $1s^{-1}3d$ excitation to this group of $2p^{-2}3d$ states. The splitting between the $2p^{-2}4p$ and $2p^{-2}3d$ states in our calculation is smaller than the splitting between the islands B and C. This disagreement can be explained with the fact that we consider a single geometry with a fixed number of water molecules in the first solvation shell. Moreover, we do not theoretically account for the effect of distant solvent shells. We assume that the transitions to the $2p^{-2}3d$ states with kinetic energies between 2982 and 2983 eV have negligible Auger rates since no additional experimental features are observed.

Another argument supporting the assignment of feature C to the $1s^{-1}3d \rightarrow 2p^{-2}3d$ Auger transition is the energy difference between the spectral features A and C. Feature A originates from electron transfer processes from water molecules (W) to the doubly core ionized potassium ion and has the configuration $K^{2+}(2p^{-2}3d)W^{-1}$. The lowest ionization potential of liquid water is about 11.16 eV[28] which matches well the observed A-C splitting. Thus, the above energetic arguments corroborate the attribution of island C as originating from resonant Auger decay to the K^{2+} $2p^{-2}3d$ final states.

In the computed $Cl^0[2p^{-2}nl](H_2O)_6$ spectrum there are two groups of states split by about 7 eV (Fig. 3(c)) which correspond to the $2p^{-2}(^1S)4p$ and $2p^{-2}(^1D)4p$ final states. The splitting between these two groups is in good agreement with the experimentally observed splitting between the dispersive features on the high kinetic energy sides of the ^1S and ^1D main peaks. Consequently, we assign the dispersive features on Fig. 3(a) to the $1s^{-1}4p \rightarrow 2p^{-2}(^1S, ^1D)4p$ resonant Auger transitions of Cl^-_{aq}.

In summary, we studied the electronic structure of aqueous solution of KCl at the K-edges of both $K^+{}_{aq}$ and $Cl^-{}_{aq}$ by combining x-ray absorption and Auger electron spectroscopy in the tender x-ray regime, and *ab initio* calculations. The Auger electron spectra of the two ions exhibit features of normal and resonant Auger processes. The spectator resonant Auger decay following the $1s^{-1}4p$ excitation proceeds similarly for both aqueous K^+ and Cl^- resulting in dispersive lines with maxima close to the normal Auger features. However, there is a clear difference between the two ions due to the non-negligible excitation of the dipole-forbidden $1s^{-1}3d$ state of K^+ in solution. The spectator Auger decay of this state produces an additional feature which is well separated from the remaining Auger features. These results are an important first step in the study of the chains of relaxation steps triggered by x-ray photoabsorption in liquids. The Auger processes considered here are inevitably followed by multiple intra- and interatomic electronic decays, such as interatomic Coulombic decay (ICD) and electron-transfer mediated decay (ETMD)[4,15]. As a result of the latter processes, genotoxic free radicals and slow electrons are formed in the vicinity of the metal center. The magnitude of the damage inflicted upon the environment and the energies of the emitted electrons depend on the initial Auger step, and can therefore be controlled by tuning the energy of the radiation. Consequently, the results of this work can have implications in understanding radiation chemistry and radiation damage in biologically relevant systems in which metallic centers are ubiquitous.

Acknowledgement

We thank Prof. Nobuhiro Kosugi and Dr. Matjaž Žitnik for the fruitful discussions. Experiments were performed at the GALAXIES beamline, SOLEIL Synchrotron, France (Proposal No. 20140160). The authors are grateful to the SOLEIL staff for assistance during the beamtime. This project has received funding from the Research Executive Agency (REA) under the European Union's Horizon 2020 research and innovation programme Grant agreement No. 705515. Campus France and the PHC SIAM exchange program are acknowledged for financial support (project No. 38282QB). L. S. Cederbaum and N. V. Kryzhevoi acknowledge the financial support of the European Research Council (ERC) (Advanced Investigator Grant No. 692657) and the Deutsche Forschungsgemeinschaft (DFG research unit 1789).

Supporting Information Available

- suppinfo.pdf: contains 1) the radial density distributions of the core excited states of the bare ions; 2) partial cross sections and charge transfer time extracted from the experimental 2D map near the Cl 1s edge.

References

(1) Smith, J. W.; Saykally, R. J. Soft X-ray Absorption Spectroscopy of Liquids and Solutions. *Chem. Rev.* **2017**, *117*, 13909–13934, PMID: 29125751.

(2) O'Neill, P.; Stevens, D. L.; Garman, E. F. Physical and chemical considerations of damage induced in protein crystals by synchrotron radiation: a radiation chemical perspective. *J. Synchrotron Radiat.* **2002**, *9*, 329–332.

(3) Carugo, O.; Carugo, K. D. When X-rays modify the protein structure: radiation damage at work. *Trends Biochem. Sci.* **2005**, *30*, 213–219.

(4) Stumpf, V.; Gokhberg, K.; Cederbaum, L. S. The role of metal ions in X-ray-induced photochemistry. *Nat. Chem.* **2016**, *8*, 237–241.

(5) Stoychev, S. D.; Kuleff, A. I.; Tarantelli, F.; Cederbaum, L. S. On the interatomic electronic processes following Auger decay in neon dimer. *J. Chem. Phys.* **2008**, *129*, 074307.

(6) Demekhin, P. V.; Scheit, S.; Stoychev, S. D.; Cederbaum, L. S. Dynamics of interatomic Coulombic decay in a Ne dimer following the $K{-}L_1L_{2,3}(^1P)$ Auger transition in the Ne atom. *Phys. Rev. A* **2008**, *78*, 043421.

(7) Demekhin, P. V.; Chiang, Y.-C.; Stoychev, S. D.; Kolorenč, P.; Scheit, S.; Kuleff, A. I.; Tarantelli, F.; Cederbaum, L. S. Interatomic Coulombic decay and its dynamics in NeAr following K-LL Auger transition in the Ne atom. *J. Chem. Phys.* **2009**, *131*, 104303.

(8) Ouchi, T.; Sakai, K.; Fukuzawa, H.; Higuchi, I.; Demekhin, P. V.; Chiang, Y.-C.; Stoychev, S. D.; Kuleff, A. I.; Mazza, T.; Schöffler, M. et al. Interatomic Coulombic decay following Ne 1s Auger decay in NeAr. *Phys. Rev. A* **2011**, *83*, 053415.

(9) Miteva, T.; Chiang, Y.-C.; Kolorenč, P.; Kuleff, A. I.; Cederbaum, L. S.; Gokhberg, K. The effect of the partner atom on the spectra of interatomic Coulombic decay triggered by resonant Auger processes. *J. Chem. Phys.* **2014**, *141*, 164303.

(10) Travnikova, O.; Marchenko, T.; Goldsztejn, G.; Jänkälä, K.; Sisourat, N.; Carniato, S.; Guillemin, R.; Journel, L.; Céolin, D.; Püttner, R. et al. Hard-X-Ray-Induced Multistep Ultrafast Dissociation. *Phys. Rev. Lett.* **2016**, *116*, 213001.

(11) Gokhberg, K.; Kolorenč, P.; Kuleff, A. I.; Cederbaum, L. S. Site- and energy-selective slow-electron production through intermolecular Coulombic decay. *Nature* **2014**, *505*, 661–663.

(12) Trinter, F.; Schöffler, M. S.; Kim, H.-K.; Sturm, F. P.; Cole, K.; Neumann, N.; Vredenborg, A.; Williams, J.; Bocharova, I.; Guillemin, R. et al. Resonant Auger decay driving intermolecular Coulombic decay in molecular dimers. *Nature* **2014**, *505*, 664–666.

(13) Pokapanich, W.; Bergersen, H.; Bradeanu, I. L.; Marinho, R. R. T.; Lindblad, A.; Legendre, S.; Rosso, A.; Svensson, S.; Björneholm, O.; Tchaplyguine, M. et al. Auger Electron Spectroscopy as a Probe of the Solution of Aqueous Ions. *J. Am. Chem. Soc.* **2009**, *131*, 7264–7271.

(14) Pokapanich, W.; Kryzhevoi, N. V.; Ottosson, N.; Svensson, S.; Cederbaum, L. S.; Öhrwall, G.; Björneholm, O. Ionic-charge dependence of the intermolecular Coulombic decay time-scale for aqueous ions probed by the core-hole clock. *J. Am. Chem. Soc.* **2011**, *133*, 13430.

(15) Unger, I.; Seidel, R.; Thürmer, S.; Pohl, M. N.; Aziz, E. F.; Cederbaum, L. S.; Muchová, E.; Slavíček, P.; Winter, B.; Kryzhevoi, N. V. Observation of electron-transfer-mediated decay in aqueous solution. *Nat. Chem.* **2017**, *9*, 708.

(16) Céolin, D.; Kryzhevoi, N. V.; Nicolas, C.; Pokapanich, W.; Choksakulporn, S.; Songsiriritthigul, P.; Saisopa, T.; Rattanachai, Y.; Utsumi, Y.; Palaudoux, J. et al. Ultrafast Charge Transfer Processes Accompanying KLL Auger Decay in Aqueous KCl Solution. *Phys. Rev. Lett.* **2017**, *119*, 263003.

(17) Goldsztejn, G.; Marchenko, T.; Ceolin, D.; Journel, L.; Guillemin, R.; Rueff, J.-P.; Kushawaha, R. K.; Puttner, R.; Piancastelli, M. N.; Simon, M. Electronic state-lifetime interference in resonant Auger spectra: a tool to disentangle overlapping core-excited states. *Phys. Chem. Chem. Phys.* **2016**, *18*, 15133–15142.

(18) Céolin, D.; Ablett, J.; Prieur, D.; Moreno, T.; Rueff, J.-P.; Marchenko, T.; Journel, L.; Guillemin, R.; Pilette, B.; Marin, T. et al. Hard X-ray photoelectron spectroscopy on

the {GALAXIES} beamline at the {SOLEIL} synchrotron. *J. Electron Spectrosc. Relat. Phenom.* **2013**, *190, Part B*, 188 – 192.

(19) Rueff, J.-P.; Ablett, J. M.; Céolin, D.; Prieur, D.; Moreno, T.; Balédent, V.; Lassalle-Kaiser, B.; Rault, J. E.; Simon, M.; Shukla, A. The GALAXIES beamline at the SOLEIL synchrotron: inelastic X-ray scattering and photoelectron spectroscopy in the hard X-ray range. *J. Synchrotron Rad.* **2015**, *22*, 175–179.

(20) Russek, A.; Mehlhorn, W. Post-collision interaction and the Auger lineshape. *J. Phys. B At. Mol. Opt. Phys.* **1986**, *19*, 911.

(21) Guillemin, R.; Sheinerman, S.; Püttner, R.; Marchenko, T.; Goldsztejn, G.; Journel, L.; Kushawaha, R. K.; Céolin, D.; Piancastelli, M. N.; Simon, M. Postcollision interaction effects in KLL Auger spectra following argon $1s$ photoionization. *Phys. Rev. A* **2015**, *92*, 012503.

(22) Sugiura, C. Influence of coordinating water on the chlorine K absorption spectra of hydrated metal dichlorides: MgCl2âŃĚ6H2O and SrCl2âŃĚ6H2O. *J. Chem. Phys.* **1982**, *77*, 681–682.

(23) Shadle, S. E.; Hedman, B.; Hodgson, K. O.; Solomon, E. I. Ligand K-edge x-ray absorption spectroscopic studies: metal-ligand covalency in a series of transition metal tetrachlorides. *J. Am. Chem. Soc.* **1995**, *117*, 2259–2272.

(24) Hertlein, M. P.; Adaniya, H.; Amini, J.; Bressler, C.; Feinberg, B.; Kaiser, M.; Neumann, N.; Prior, M. H.; Belkacem, A. Inner-shell ionization of potassium atoms ionized by a femtosecond laser. *Phys. Rev. A* **2006**, *73*, 062715.

(25) Krause, M. O.; Oliver, J. H. Natural widths of atomic K and L levels, Kα X-ray lines and several KLL Auger lines. *J. Phys. Chem. Ref. Data* **1979**, *8*, 329–338.

(26) Miteva, T.; Wenzel, J.; Klaiman, S.; Dreuw, A.; Gokhberg, K. X-Ray absorption spectra of microsolvated metal cations. *Phys. Chem. Chem. Phys.* **2016**, *18*, 16671–16681.

(27) Céolin, D.; Marchenko, T.; Guillemin, R.; Journel, L.; Kushawaha, R. K.; Carniato, S.; Huttula, S.-M.; Rueff, J. P.; Armen, G. B.; Piancastelli, M. N. et al. Auger resonant-Raman study at the Ar K edge as probe of electronic-state-lifetime interferences. *Phys. Rev. A* **2015**, *91*, 022502.

(28) Winter, B.; Weber, R.; Widdra, W.; Dittmar, M.; Faubel, M.; Hertel, I. V. Full Valence Band Photoemission from Liquid Water Using EUV Synchrotron Radiation. *J. Phys. Chem. A* **2004**, *108*, 2625–2632.